Cell Biochem Biophys (2015) 71:1643–1651
DOI 10.1007/s12013-014-0386-6

ORIGINAL PAPER

Cerium Oxide Nanoparticles Induce Oxidative Stress and Genotoxicity in Human Skin Melanoma Cells

Daoud Ali · Saud Alarifi · Saad Alkahtani · Abdullah A. AlKahtane · Abdulaziz Almalik

Published online: 14 November 2014

Abstract Extensive applications of cerium oxide (CeO_2) nanoparticles require a better understanding of their possible effects on human health. However, data demonstrating the effect of CeO_2 nanoparticles on the human skin melanoma cell remain scanty. In the current study, we determined the mechanism through which CeO_2 nanoparticles (APS <25 nm) induce toxicity in human skin melanoma cells (A375). The MTT [3-(4,5-dimethylthiazol-2-yl)-2,5-diphenyltetrazolium bromide] and neutral red uptake assays showed concentration and time-dependent cytotoxicity of CeO_2 nanoparticles in A375 cells. CeO_2 nanoparticles significantly induced the generation reactive oxygen species (ROS) and malondialdehyde, superoxide dismutase, and decreased glutathione levels in A375 cells. It was also observed that the CeO_2 nanoparticles induced chromosomal condensation and caspase-3 activity. CeO_2 nanoparticles exposed cells revealed the formation of DNA double-strand breakage as measured by percent tail DNA and olive tail moment through comet assay. The decline of cell viability, production of ROS, and DNA damage in A375 cells specifies that CeO_2 nanoparticles have less capable to induce cyto and genotoxicity.

Keywords CeO_2 nanoparticles · A375 cells · Oxidative stress · Apoptosis · DNA damage

D. Ali (✉) · S. Alarifi · S. Alkahtani · A. A. AlKahtane
Department of Zoology, College of Science, King Saud University, BOX 2454, Riyadh 11451, Saudi Arabia
e-mail: aalidaoud@ksu.edu.sa; daudali.ksu12@yahoo.com

A. Almalik
King Abdulaziz City for Science and Technology, Riyadh, Saudi Arabia

Introduction

The CeO_2 nanoparticles are widely employed in ultraviolet absorbents, solar cells, solid fuel cells, automotive catalytic converters, gas sensors, oxygen pumps, and glass ceramic applications [1]. Due to wide use of CeO_2 nanoparticles in industries, concerns about their potential toxic effects in humans and environmental effects have increased. Frohlich and Roblegg [2] reported that CeO_2 nanoparticles can enter the general circulation through the respiratory mucosal barriers, the gastrointestinal mucosal barrier, and the skin barriers, after which they may invade all tissues and organs via the blood due to their physical and chemical characteristics. Some researchers reported that CeO_2 nanoparticles are cytotoxic to various tissues and cells [3, 4]. However, the molecular mechanisms by which CeO_2 nanoparticles induce toxicity remain unexplored.

Due to growing of CeO_2 nanoparticles applications, there is an increasing risk of environmental exposure to nanomaterials. Their potential impacts are still a matter of investigation and our actual knowledge on the effects of nano-sized pollutants on biological systems remains incomplete [5, 6]. These effects need to be assessed in order to provide a scientific basis for a safe development of nanotechnology. Due to their small size, nanoparticles may cross biological barriers to reach different tissues and according to their surface and size, accumulation of metal nanoparticles was previously observed in many different organs [7].

The skin is the largest organ of the body and could serve an important role in the human body. The genotoxic potential of nanomaterial is of particular concern since the changes of the genetic material have potential for cell death, tissue malfunction, cancer development, and reproductive adverse effects. Wang et al. [8] had been reported

that nanoparticles induced oxidative stress as assessed by increasing membrane lipid peroxidation (LPO), reactive oxygen species (ROS), and decreasing intracellular glutathione (GSH). Oxidative stress plays an important role in cellular signaling, inflammatory, and genotoxic and proliferative responses [9, 10]. We evaluated the oxidative stress biomarkers including GSH, ROS, and LPO in response to CeO_2 nanoparticles exposure.

Therefore, the current study was designed to assess the cellular toxicity and genotoxic potential of CeO_2 nanoparticles in human skin melanoma cells as well as to understand its possible mechanism.

Materials and Methods

Chemicals and Reagents

Cerium oxide (CeO_2) nanoparticles (Product No. 544841 and APS <25 nm), glutathione (GSH), 5,5-dithio-bis-(2-nitrobenzoic acid) (DTNB), MTT [3-(4,5-dimethylthiazol-2-yl)-2,5-diphenyltetrazolium bromide], 2,7-dichlorofluorescin diacetate (DCFH-DA), neutral red dye, and 4′,6-diamidino-2-phenylindole (DAPI) were obtained from Sigma-Aldrich (St. Louis, MO). Fetal bovine serums, penicillin–streptomycin, and DMEM/F-12 medium were purchased from Invitrogen Co. (Carlsbad, CA, USA). All other chemicals were of high purity and available from commercial sources.

CeO_2 Nanoparticles Preparation and Characterization

CeO_2 nanoparticles were suspended in media at a concentration of 1 mg/ml. Nanoparticles suspension was sonicated at 40 W for 15 min. The average hydrodynamic size of CeO_2 nanoparticles in media was determined by dynamic light scattering (DLS) (Nano-ZetaSizer-HT, Malvern Instrument, UK). Samples for transmission electron microscopy (TEM) analysis were prepared by drop-coating CeO_2 nanoparticles solution on carbon-coated copper TEM grids. The films on the TEM grids were allowed to dry prior to measurement. TEM measurements were performed on a JEOL model 2100 F instruments operated at an accelerating voltage of 200 kV.

Cell Culture and Exposure of CeO_2 Nanoparticles

Human skin melanoma cells (A375) were procured from American type culture collection Rockville, MD, USA and it was cryopreserved and sub-cultured in our laboratory and was used to determine the cytotoxicity against CeO_2 nanoparticles. Cells were cultured in DMEM/F-12 medium supplemented with 10 % FBS and 100 U/ml penicillin–streptomycin at 5 % CO_2 and 37 °C. At 85 % confluence, cells were harvested by using 0.25 % trypsin and were sub-cultured into 75 cm^2 flasks, 6-well plates and 96-well plates according to experiments. Cells were allowed to attach the surface for 24 h prior to treatment. CeO_2 nanoparticles were suspended in cell culture medium and diluted to appropriate concentrations (0, 20, 40, 80, and 120 μg/ml). The appropriate dilutions of CeO_2 nanoparticles were sonicated using a sonicator bath at room temperature for 10 min at 40 W to avoid particle agglomeration before exposure to the cells. Cells not exposed to CeO_2 nanoparticles served as control in each experiment.

Cell Morphology

The morphology of human skin melanoma cells A375 cells was observed after exposure of CeO_2 nanoparticles for 24 and 48 h using a phase contrast microscope (Leica DMIL).

MTT Assay

MTT assay was used to investigate mitochondrial function as described by Alarifi et al. [11]. Briefly, 1×10^4 cells/well were seeded in 96-well plates and exposed to different concentrations (0, 20, 40, 80, and 120 μg/ml) of CeO_2 nanoparticles for 24 and 48 h. At the end of the exposure, culture media were replaced with new media containing MTT solution (0.5 mg/ml) and incubated for 4 h at 37 °C. As a result, formazan crystal was formed and it was dissolved in DMSO. The plates were kept on shaker for 10 min at room temperature and then analyzed at 530 nm using multiwell microplate reader (Omega Fluostar). Untreated sets were also run under identical conditions and served as controls.

NRU Assay

The neutral red uptake (NRU) assay was done according to the method of Ali et al. [12]. After the exposure of CeO_2 nanoparticles, medium was discarded and 100 μl of neutral red dye (50 μg/ml) dissolved in serum-free medium was added to each well. After incubation at 37 °C for 3 h, cells were washed with a solution of 0.5 % formaldehyde and 1 % $CaCl_2$. The accumulated dye was extracted with 50 % ethanol containing 1 % (v/v) acetic acid and plates were kept for 20 min on a shaker. The absorbance was recorded at 540 nm by using multiwall microplate reader (Omega Fluostar).

Measurement of Intracellular ROS

ROS generation was assessed in A375 cells after exposure of different concentrations (0, 20, 40, 80, and 120 μg/ml) of CeO_2 nanoparticles by using 2,7-dichlorofluorescin

diacetate (DCFH-DA) dye as fluorescence agent [13]. ROS production was studied by two methods: fluorometric analysis and microscopic fluorescence imaging. The fluorometric analysis, cells (1×10^4 per well) were seeded in 96-well black bottom culture plates and allowed to adhere them for 24 h in a CO_2 incubator at 37 °C. Then A375 cells were exposed to the above concentrations of CeO_2 nanoparticles for 24 and 48 h. On the completion of respective exposure periods, cells were incubated with DCFH-DA (10 mM) for 30 min at 37 °C. The reaction mixture was aspirated and replaced by 200 µl of PBS in each well. The plates were kept on shaker for 10 min at room temperature in the dark. Fluorescence intensity was measured using multiwell microplate reader (Omega Fluostar) at excitation wavelength 485 nm and at emission wavelength 528 nm, and values were expressed as percent of fluorescence intensity relative to control wells.

A parallel set of cells (5×10^4 per well) were analyzed for intracellular fluorescence using upright fluorescence microscope equipped with a CCD cool camera (Nikon Eclipse 80i equipped with Nikon DS-Ri1 12.7 mega pixel camera).

Oxidative Stress Biomarkers

The cells at a final density of $\sim 6 \times 10^6$ in a 75 cm^2 culture flask were exposed to CeO_2 nanoparticles (0, 20, 40, 80, and 120 µg/ml) for 24 and 48 h. After exposure, the cells were scraped and washed twice with chilled 1× PBS. The harvested cell pellets were lysed in cell lysis buffer [20 mM Tris–HCl (pH 7.5), 150 mM NaCl, 1 mM Na_2EDTA, 1 % Triton, and 2.5 mM sodium pyrophosphate]. The cells were centrifuged at 15000 g for 10 min at 4 °C and the supernatant (cell extract) was maintained on ice until assayed for oxidative stress biomarkers. Protein content was measured by the method of Bradford [14], using bovine serum albumin as the standard.

Lipid Peroxidation (LPO) Assay

The membrane LPO was estimated by measuring the formation of malondialdehyde (MDA) using the method of Ohkawa et al. [15]. MDA is one of the products of membrane LPO. A mixture of 0.1 ml cell extract and 1.9 ml of 0.1 M sodium phosphate buffer (pH 7.4) was incubated at 37 °C for 1 h. The incubation mixture, after precipitation with 5 % TCA, was centrifuged (2300 g for 15 min at room temperature) and the supernatant collected. Then 1.0 ml of 1 % TBA was added to the supernatant and placed in the boiling water for 15 min. After cooling to room temperature, absorbance of the mixture was taken at 532 nm and expressed in *n* mol MDA/h/mg protein using a molar extinction coefficient of 1.56×10^5/M/cm.

GSH Estimation

GSH level was quantified using Ellman's reagent [16]. The assay mixture contained phosphate buffer, DTNB, and cell extract. The reaction was monitored at 412 nm and the amount of GSH was expressed in terms of *n* mol GSH/mg protein.

Measurement of SOD

SOD activity was estimated by employing a method described by Alarifi et al. [11]. The assay mixture contained sodium pyrophosphate buffer, nitroblue tetrazolium, phenazine methosulphate, reduced nicotinamide adenine dinucleotide (NADH), and the required volume of cell extract. One unit of SOD enzyme activity is defined as the amount of enzyme required for inhibiting the chromogen production (560 nm) by 50 % in 1 min under assay conditions and expressed as specific activity in units/min/mg protein.

DAPI Staining for Chromosome Condensation

Chromosome condensation in A375 cells due to CeO_2 nanoparticles exposure was observed by 4′,6-diamidino-2-phenylindole (DAPI) staining according to the method described by Alarifi et al. [11]. DAPI solution was used to stain the exposed cells in eight chamber slides and the slides were incubated for 10 min in the dark at 37 °C. Images of the nucleus were captured using a fluorescence microscope (Nikon).

Caspase-3 Assay

The activity of caspase-3 was determined from the cleavage of the caspase-3 substrate (*N*-acetyl-DEVD-*p*-nitroaniline). The *p*-nitroaniline was used as the standard. Cleavage of the substrate was monitored at 405 nm, and the specific activity was expressed in picomoles of the product (nitroaniline) per min/mg of protein.

Determination of DNA Damage

The alkaline single cell gel electrophoresis was performed as a three layer procedure with slight modification [17]. In brief, 70,000 cells/well were seeded in a six-well plate. After 24 h of seeding, cells were treated with different concentrations of CeO_2 nanoparticles for 24 and 48 h. After treatment, the A375 cells were trypsinized and suspended in DMEM, and cell suspension was centrifuged at 1200 rpm at 4 °C for 5 min. The cell pellet was finally suspended in chilled phosphate buffer saline for comet assay. The samples showing cell viability higher than 84 % were further processed for comet assay. In brief, about 15 µl of cell suspension (approx. 20,000 cells) was mixed with 85 µl of 0.5 %

low melting point agarose and layered on one end frosted plain glass slide, pre-coated with a layer of 200 µl normal agarose (1 %). Thereafter, it was covered with a third layer of 100 µl low melting point agarose. After solidification of the gel, the slides were immersed in lysing solution (2.5 M NaCl, 100 mM Na_2EDTA, 10 mM Tris pH 10 with 10 % DMSO, and 1 % Triton X-100 added fresh) overnight at 4 °C. The slides were then placed in a horizontal gel electrophoresis unit. Fresh cold alkaline electrophoresis buffer (300 mM NaOH, 1 mM Na_2EDTA, and 0.2 % DMSO, pH 13.5) was poured into the chamber and left for 20 min at 4 °C for DNA unwinding and conversion of alkali-labile sites to single-strand breaks. Electrophoresis was carried out using the same solution at 4 °C for 20 min, at 15 V (0.8 V/cm) and 300 mA. The slides were neutralized gently with 0.4 M tris buffer at pH 7.5 and stained with 75 µl ethidium bromide (20 µg/ml). For positive control, the A375 cells were treated with 100 µM H_2O_2 for 10 min at 4 °C. Two slides were prepared from each well (per concentration), and 50 cells per slide (100 cells per concentration) were scored randomly and analyzed using an image analysis system (Komet-5.0, Kinetic Imaging, Liverpool UK) attached to fluorescence microscope (DMLB, Leica, Germany) equipped with appropriate filters. The parameters e.g., percent tail DNA (i.e. % tail DNA = 100 − % head DNA) and olive tail moment were selected for quantification of DNA damage in A375 cells as determined by the software.

Statistical Analysis

At least three independent experiments were carried out in duplicates for each evaluation. Data were expressed as mean (±SE) and analyzed by one-way analysis of variance (ANOVA). The p value less than 0.01 was considered statistically significant.

Results

CeO_2 Nanoparticles

The average size of CeO_2 nanoparticles is around 38 nm (Fig. 1a). The figure exhibits that the most of the particles were in rectangular shape. The average hydrodynamic size and zeta potential of CeO_2 nanoparticles in media determined by DLS were 186.20 nm and −11.7 mV, respectively.

Morphological Alterations of A375 Cells

Figure 2 shows the comparative morphology of untreated and CeO_2 nanoparticles treated A375 cells. A375 cells exposed to 80 µg/ml CeO_2 nanoparticles altered into spherical shape and detached from surface (Fig. 2b).

CeO_2 Nanoparticles Induced Cytotoxicity in A375 Cells

We examined the mitochondrial function (MTT reduction) and lysosomal activity (NR uptake) as cytotoxicity end points. MTT results demonstrated a dose and time-dependent cytotoxicity after exposure to CeO_2 nanoparticles in A375 cells (Fig. 3a).The result of NPU assay is shown in Fig. 3b. The result showed concentration and time-dependent decline in viability of cells exposed to CeO_2 nanoparticles for 24 and 48 h.

CeO_2 Nanoparticles Induced ROS Generation and Oxidative Stress

The ability of CeO_2 nanoparticles to induce oxidative stress was evaluated by measuring the levels of ROS, LPO, GSH, and SOD in A375 cells. Results showed that CeO_2 nanoparticles induced the intracellular ROS generation in A375 cells (Fig. 4). CeO_2 nanoparticles induced oxidative stress was further evidenced by depletion of GSH (Fig. 5a) and elevation of LPO, and SOD with concentrations and time of CeO_2 nanoparticles exposure (Fig. 5b, c).

Induction of Chromosomal Condensation and Caspase-3 Activity by CeO_2 Nanoparticles

Chromatin condensation was determined by DAPI staining. A375 cells treated with CeO_2 nanoparticles at above mentioned concentration for 48 h produced chromatin condensation (Fig. 6a, b).

Caspase-3, which plays a key role in the apoptotic pathway of cells, was induced following the treatment with CeO_2 nanoparticles (Fig. 6c). Cells were treated with CeO_2 nanoparticles (20, 40, and 80 µg/ml) for 24 and 48 h, the activity of caspase-3 was increased in a concentration and time-dependent manner.

DNA Strand Breakage

The DNA damage was measured as % tail DNA and olive tail moment in the control as well as CeO_2 nanoparticles treated cells. The cells treated to different concentrations of CeO_2 nanoparticles, exhibited significantly ($p > 0.01$) higher DNA damage in cells than control groups. The highest DNA damage was recorded in A375 cells at 80 µg/ml CeO_2 nanoparticles (Fig. 7).

Discussion

The current study was designed to assess the cytotoxic and genotoxic of CeO_2 nanoparticles using A375 cells with

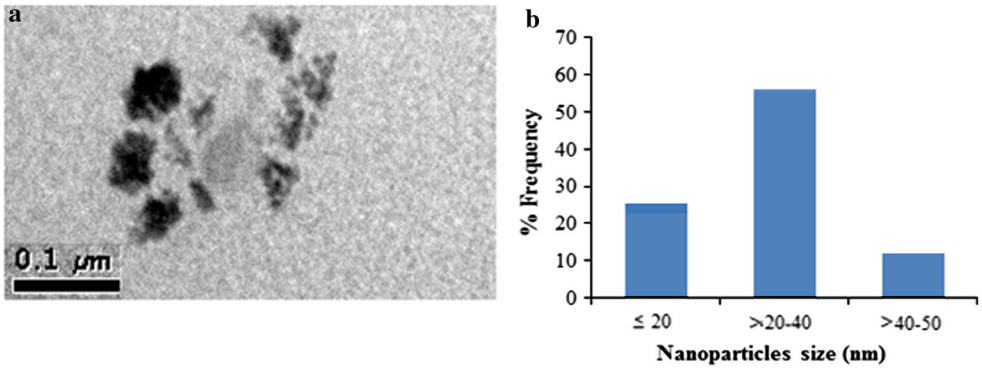

Fig. 1 Characterization of CeO_2 nanoparticles. **a** TEM image. **b** The size distribution histogram generated using TEM image

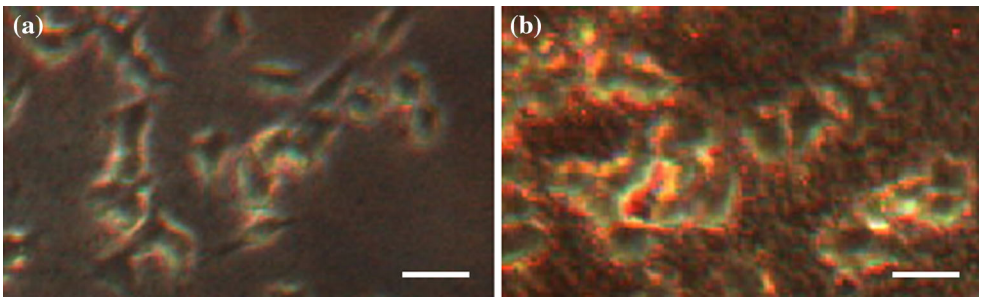

Fig. 2 Morphology of A375 cells. **a** Control, **b** treated at 80 μg/ml of CeO_2 nanoparticles. *Scale bars* (*thick solid line*) 100 μm

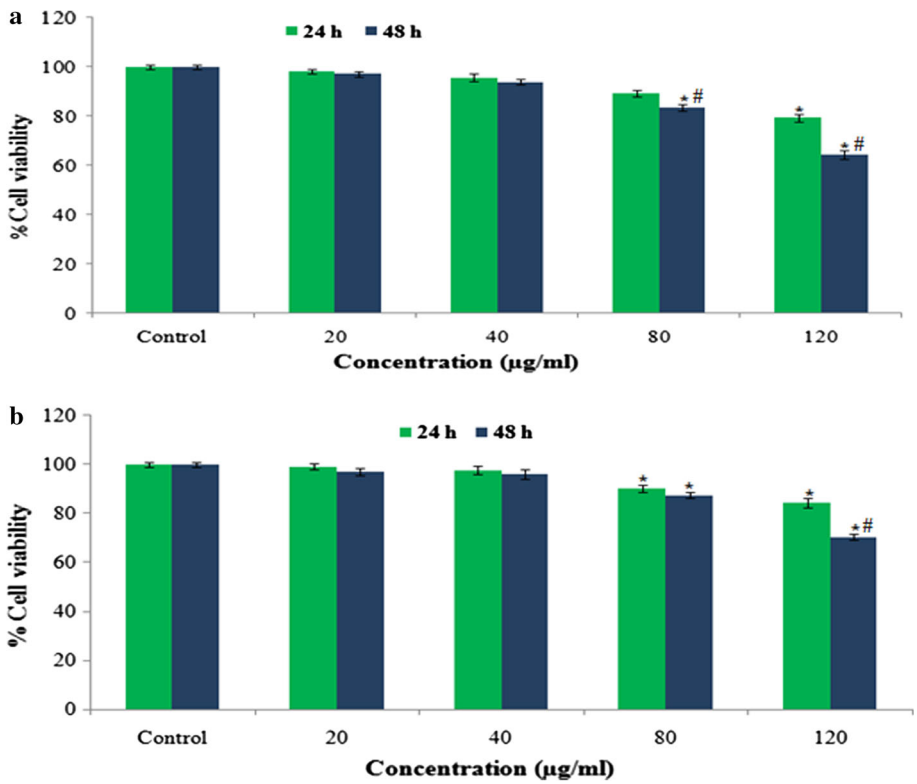

Fig. 3 Percentage cell viability at different concentrations of CeO_2 nanoparticles in A375 cells for 24 h and 48 h, as assessed by **a** MTT assay **b** NRU assay. Each value represents the mean ± SE of three experiments.*$p < 0.01$ versus control. #$p < 0.01$ versus between durations as within concentration

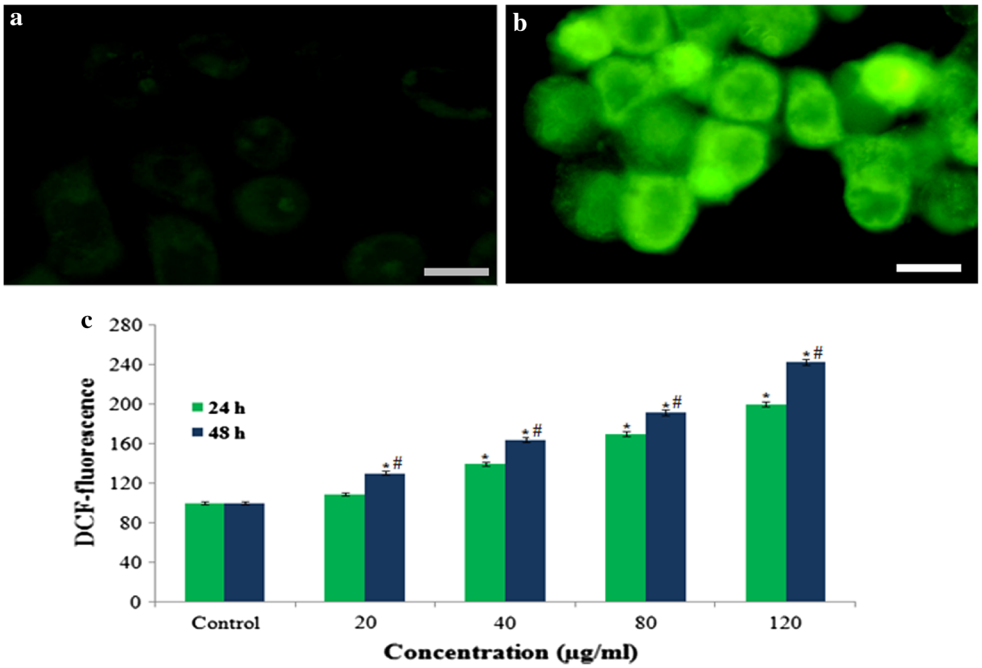

Fig. 4 CeO_2 nanoparticles induced ROS production in A375 cells. **a** Control , **b** at 80 µg/ml of CeO_2 nanoparticles. **c** Percentage of ROS generation at different concentrations of CeO_2 nanoparticles in A375 cells. Images were snapped in Nikon phase contrast cum fluorescence microscope (model 80i). Each value represents the mean ± SE of three experiments.*$p < 0.01$ versus control. #$p < 0.01$ versus between durations as within concentration. *Scale bars* (*thick solid line*) 50 µm

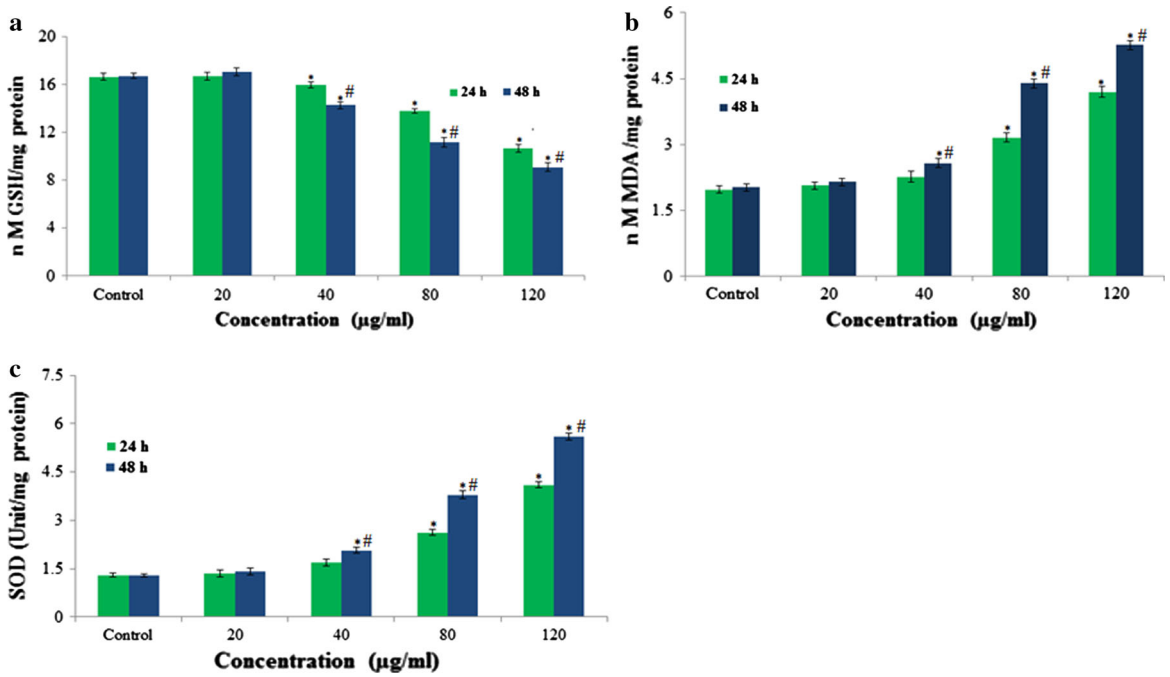

Fig. 5 **a** Levels of GSH. **b** Lipid peroxides. **c** SOD in A375 cells after exposure of CeO_2 nanoparticles for 24 and 48 h. Each value represents the mean ± SE of three experiments.*$p < 0.01$ versus control. #$p < 0.01$ versus between durations as within concentration

concerns on the possible adverse effects of CeO_2 nanoparticles along with their toxic potential. Our results indicate that CeO_2 nanoparticles have low cytotoxic and genotoxic effects in A375 cells. The results also showed that the mode of cell death was apoptosis via ROS triggered mitochondrial pathway as evidenced by cleavage of

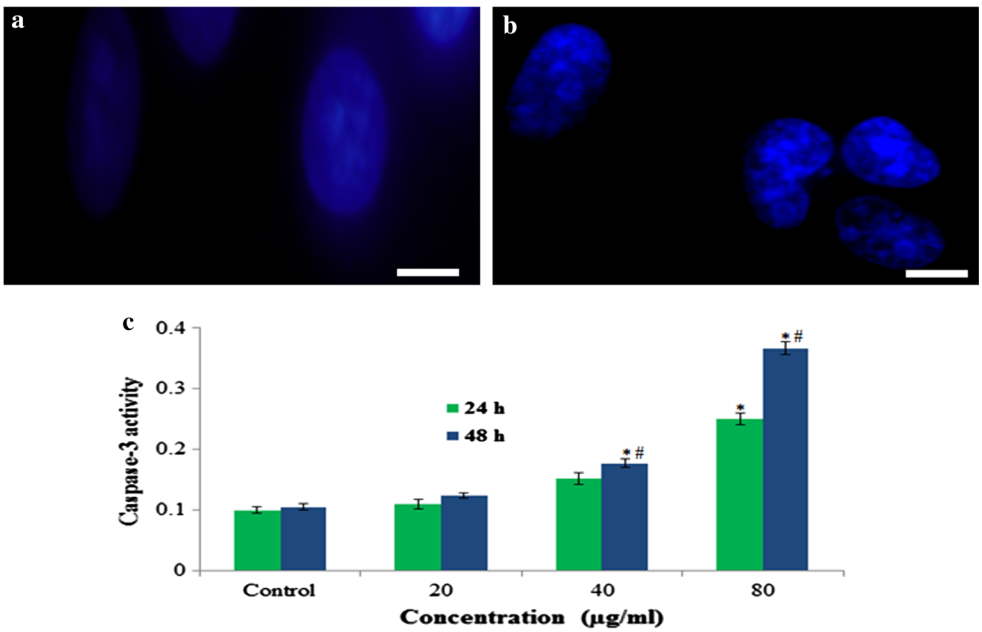

Fig. 6 Chromosomal condensation and induction of caspase-3 activity in A375 cells after exposure of CeO_2 nanoparticles for 24 and 48 h. **a** Control (viable) cell, **b** at 80 µg/ml of CeO_2 nanoparticles. **c** Caspase-3 activity. Each value represents the mean ± SE of three experiments. $*p < 0.01$ versus control. $\#p < 0.01$ versus between durations as within concentration. *Scale bars* (*thick solid line*) 50 µm

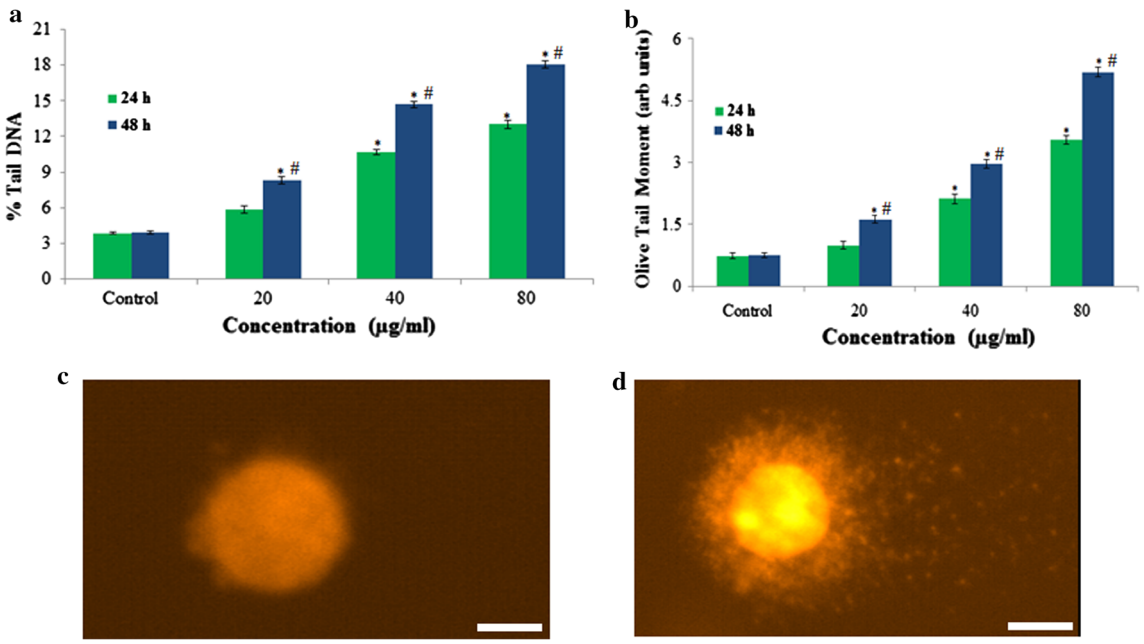

Fig. 7 DNA damage in A375 cells at different concentrations of CeO_2 nanoparticles. **a** Tail DNA (%). **b** Olive tail moment. **c** Control cell. **d** Exposed cell. Each value represents the mean ± SE of three experiments. $*p < 0.01$ versus control. $\#p < 0.01$ versus between durations as within concentration. *Scale bars* (*thick solid line*) 20 µm

caspase-3 and chromosome condensation. The size of CeO_2 nanoparticles had been characterized by DLS and TEM prior to study its toxicity in A375 cells. However, the size obtained from DLS was more than the size measured by TEM. The difference in size is due to the fact that different size determination methods give different results based on these principles used; first, DLS measures Brownian motion and subsequent size distribution of an ensemble collection of particles in solution and gives mean hydrodynamic diameter, which is usually larger than TEM diameter as it includes a few solvent layers; second, during DLS measurement, there is a tendency of particles to agglomerate in the aqueous state thereby giving the size of clustered particles rather than individual particles.

The intervention of some nanoparticles with used cytotoxicity assays has been well reported in the literature.

Therefore, it has been suggested that the cytotoxicity of nanoparticles should be assessed with two or more independent test systems for validating the findings [18]. We have evaluated the cytotoxicity of CeO_2 nanoparticles by two different assays e.g., the MTT and NR uptake to increase the strength of the data. In the present study, CeO_2 nanoparticles induced cytotoxicity in dose and time-dependent manner. The induction of cytotoxicity as observed in the present study is in concordance with the findings of Horie et al. [19] in the human skin keratinocyte for CeO_2 nanoparticles.

Nel et al. [20] had reported that LPO and oxidative stress is one of the most important mechanisms of toxicity related to nanoparticles. This has been attributed to their small size and large surface area which is generally thought to produce ROS and oxidative stress [21]. The CeO_2 nanoparticles in our study also produced intracellular ROS when examined by the cell permeable dye DCFH-DA. ROS typically include the superoxide radical, hydrogen peroxide, and the hydroxyl radical which cause damage to cellular components including DNA damage and ultimately apoptotic cell death [22, 23]. This observation is consistent with the earlier studies which have shown similar effects on human SMMC-7721 cells [24].

We detected an increase in LPO and SOD, while decrease antioxidant GSH level in A375 cells after exposure to CeO_2 nanoparticles, which represents marker of oxidative stress. LPO can further give rise to more free radicals and damage biomolecules like DNA, protein, and lipids in conjunction with ROS. The depletion of GSH in CeO_2 nanoparticles exposed cells combined with the increased level of LPO and SOD indicates that oxidative stress may be the primary mechanism for toxicity of CeO_2 nanoparticles in A375 cells. CeO_2 nanoparticles can also lead to free radicals generation after their interaction with cells components, like mitochondrial damage. Another way by which ROS is generated is through the activation of NADPH-oxidase enzyme which is responsible for O^{2-} production in the membrane of phagocytic cells. When free radicals come in close with the cellular organelles, they may oxidize and reduce macromolecules (DNA, lipids, and proteins) resulting in significant oxidative damage to cell. Nanoparticles induced LPO and oxidative stress leads to DNA damage and apoptosis [25]. Our results are consistent with other investigators finding, demonstrating metal oxide nanoparticles have the potential to induce DNA damage. CeO_2 nanoparticles significantly generated toxic effect in A375 cells.

CeO_2 nanoparticles induced cell death observed in this study can occur by two distinct modes—apoptosis and necrosis which can be distinguished by morphological and biochemical features. DAPI staining of CeO_2 nanoparticles treated A375 cells resulted in chromosomal condensation and fragmentation which is another morphological hallmark of apoptosis. Chen and Mikecz [26] reported that nanoparticles due to their small size are capable of reaching to the nucleus and interact with DNA. They may also exhibit an indirect effect on DNA through their ability to generate ROS. This DNA damage may either induce to carcinogenesis or cell death, thus disrupting normal cell functions. We detected the genotoxic potential of CeO_2 nanoparticles in A375 cells by comet assay which is capable of detecting single as well as double DNA strand breaks and alkali-labile sites even at low levels of DNA damage [27]. Martinez et al. [28] have been reported that ROS are involved in DNA damage causing damage to both purine and pyrimidine bases as well as the DNA backbone.

Our results demonstrate that CeO_2 nanoparticles induce apoptosis and DNA damage in human skin melanoma cells, which may be mediated through the ROS and oxidative stress.

Acknowledgments The authors would like to extend their sincere appreciation to the Deanship of Scientific Research at King Saud University for its funding of this research through the research Group Project No. RGP-VPP-180.

Conflict of interest None.

References

1. Riehemann, K., Schneider, S. W., Luger, T. A., Godin, B., Ferrari, M., & Fuchs, H. (2009). Nanomedicine-challenge and perspectives. *Angewandte Chemie International Edition, 48*, 872–897.
2. Frohlich, E., & Roblegg, E. (2012). Models for oral uptake of nanoparticles in consumer products. *Toxicology, 291*, 10–17.
3. Eom, H. J., & Choi, J. (2009). Oxidative stress of CeO_2 nanoparticles via p38-Nrf-2 signaling pathway in human bronchial epithelial cell, Beas-2B. *Toxicology Letters, 187*, 77–83.
4. Kim, I. S., Baek, M., & Choi, S. J. (2010). Comparative cytotoxicity of Al_2O_3, CeO_2, TiO_2 and ZnO nanoparticles to human lung cells. *Journal for Nanoscience and Nanotechnology, 10*, 3453–3458.
5. Singh, N., Manshian, B., Jenkins, G. J. S., Griffiths, S. M., Williams, P. M., Maffeis, T. G., et al. (2009). Nano Genotoxicology: The DNA damaging potential of engineered nanomaterials. *Biomaterials, 30*, 3891–3914.
6. Skocaj, M., Filipic, M., Petkovic, J., & Novak, S. (2011). Titanium dioxide in our everyday life; is it safe? *Radiology and Oncology, 45*, 227–247.
7. Li, Y.-F., & Chen, C. (2011). Fate and toxicity of metallic and metal-containing nanoparticles for biomedical applications. *Small (Weinheim an der Bergstrasse, Germany), 7*, 2965–2980.
8. Wang, Y., Aker, W. G., Hwang, H. M., Yedjou, C. G., Yu, H., et al. (2011). A study of the mechanism of in vitro cytotoxicity of metal oxide nanoparticles using catfish primary hepatocytes and human HepG2 cells. *Science of the Total Environment, 409*, 4753–4762.
9. van Maanen, J. M., Borm, P. J., Knaapen, A., van Herwijnen, M., Schilderman, P. A., Smith, K. R., et al. (1999). In vitro effects of coal fly ashes: Hydroxyl radical generation, iron release, and DNA damage and toxicity in rat lung epithelial cells. *Inhalation Toxicology, 11*, 1123–1141.

10. Borm, P. J., Schins, R. P., & Albrecht, C. (2004). Inhaled particles and lung cancer, part B: Paradigms and risk assessment. *International Journal of Cancer, 110*, 3–14.
11. Alarifi, S., Ali, D., Alkahtani, S., Verma, A., Ahamed, M., Ahmed, M., et al. (2013). Induction of oxidative stress, DNA damage, and apoptosis in a malignant human skin melanoma cell line after exposure to zinc oxide nanoparticles. *International Journal of Nanomedicine, 8*, 983–993.
12. Ali, D., Verma, A., Mujtaba, F., Dwivedi, A., Hans, R. K., & Ray, R. S. (2011). UVB-induced apoptosis and DNA damaging potential of chrysene via reactive oxygen species in human keratinocytes. *Toxicology Letters, 204*, 199–207.
13. Suliman, A. Y., Ali, D., Alarifi, S., Harrath, A. H., Mansour, L., & Alwasel, S. H. (2013). Evaluation of cytotoxic, oxidative stress, proinflammatory and genotoxic effect of silver nanoparticles in human lung epithelial cells. *Toxicology Environmental,*. doi:10.1002/tox.21880.
14. Bradford, M. M. (1976). A rapid and sensitive method for the quantitation of microgram quantities of protein utilizing the principle of protein-dye binding. *Analytical Biochemistry, 72*, 248–254.
15. Ohkawa, H., Ohishi, N., & Yagi, K. (1979). Assay for lipid peroxides in animal tissues by thiobarbituric acid reaction. *Analytical Biochemistry, 95*, 351–358.
16. Ellman, G. L. (1959). Tissue sulfhydryl groups. *Archives of Biochemistry and Biophysics, 82*, 70–77.
17. Ali, D., Ray, R. S., & Hans, R. K. (2010). UVA-induced cytotoxicity and DNA damaging potential of Benz (e) acephenanthrylene in human skin cell line. *Toxicology Letters, 199*(2), 193–200.
18. Monteiro-Riviere, N. A., Inman, A. O., & Zhang, L. W. (2009). Limitations and relative utility of screening assays to assess engineered nanoparticle toxicity in a human cell line. *Toxicology and Applied Pharmacology, 234*(2), 222–235.
19. Horie, M., Nishio, K., Kato, H., Fujita, K., Endoh, S., Nakamura, A., et al. (2011). Cellular responses induced by cerium oxide nanoparticles: Induction of intracellular calcium level and oxidative stress on culture cells. *Journal of Biochemistry, 150*(4), 461–471.
20. Nel, A., Xia, T., Madler, L., & Li, N. (2006). Toxic potential of materials at the nano level. *Science, 311*, 622–627.
21. Xia, T., Kovochich, M., Brant, J., Hotze, M., Sempf, J., Oberley, T., et al. (2006). Comparison of the abilities of ambient and manufactured nanoparticles to induce cellular toxicity according to an oxidative stress paradigm. *Nano Letters, 6*(8), 1794–1807.
22. Ott, M., Gogvadze, V., Orrenius, S., & Zhivotovsky, B. (2007). Mitochondria, oxidative stress and cell death. *Apoptosis, 12*, 913–922.
23. Rana, S. V. (2008). Metals and apoptosis: Recent developments. *Journal of Trace Elements in Medicine and Biology, 22*, 262–284.
24. Cheng, G., Guo, W., Han, L., Chen, E., Kong, L., Wang, L., et al. (2013). Cerium oxide nanoparticles induce cytotoxicity in human hepatoma SMMC-7721 cells via oxidative stress and the activation of MAPK signaling pathways. *Toxicology in Vitro, 27*(3), 1082–1088.
25. Kang, S. J., Kim, B. M., Lee, Y. J., & Chung, H. (2008). Titanium dioxide nanoparticles trigger p53-mediated damage response in peripheral blood lymphocytes. *Environmental and Molecular Mutagenesis, 49*, 399–405.
26. Chen, M., & von Mikecz, A. (2005). Formation of nucleoplasmic protein aggregates impairs nuclear function in response to SiO_2 nanoparticles. *Experimental Cell Research, 305*(1), 51–62.
27. Collins, A. R. (2004). The comet assay for DNA damage and repair: Principles, applications and limitations. *Molecular Biotechnology, 26*(3), 249–261.
28. Martinez, G. R., Loureiro, A. P., Marques, S. A., Miyamoto, S., Yamaguchi, L. F., Onuki, J., et al. (2003). Oxidative and alkylating damage in DNA. *Mutation Research, 544*, 115–127.